Structural Engineering and Mechanics, *Vol. 53, No. 4 (2015) 681-702*
DOI: http://dx.doi.org/10.12989/sem.2015.53.4.681

Fracture analysis and remaining life prediction of aluminium alloy 2014A plate panels with concentric stiffeners under fatigue loading

A. Ramachandra Murthy*[1], Rakhi Sara Mathew[2a], G.S. Palani[1b], Smitha Gopinath[1b] and Nagesh R. Iyer[1c]

[1]CSIR-Structural Engineering Research Centre, Taramani, Chennai, 600 113, India
[2]Saintgits College of Engineering, Pathamuttom P O, Kottayam, Kerala, 686 532, India

(Received June 12, 2014, Revised September 3, 2014, Accepted October 4, 2014)

Abstract. Fracture analysis and remaining life prediction has been carried out for aluminium alloy (Al 2014A) plate panels with concentric stiffener by varying sizes and positions under fatigue loading. Tension coupon tests and compact tension tests on 2014A have been carried out to evaluate mechanical properties and crack growth constants. Domain integral technique has been used to compute the Stress intensity factor (SIF) for various cases. Generalized empirical expressions for SIF have been derived for various positions of stiffener and size. From the study, it can be concluded that the remaining life for stiffened panel for particular size and position can be estimated by knowing the remaining life of corresponding unstiffened panel.

Keywords: stiffened panel; fracture analysis; stress intensity factor; remaining life; concentric stiffener

1. Introduction

In most of the industrial structures, the strength of structural components are generally improved by providing stiffening members such as stiffeners or stringers. The main function of a stiffener is to improve the strength and stability of the structure and to slow down or arrest the growth of cracks in the panel. Remaining life prediction of the cracked structural components in these structures is necessary for their in-service inspection, planning, repair, retrofitting, rehabilitation, requalification and health monitoring. In view of these, it is essential to use the damage tolerant design concepts for designing structural components. Practically for all the high strength materials employed in the construction of above structures/components, damage tolerant analysis can be performed using linear elastic fracture mechanics (LEFM) principles, in which case, stress intensity factor (SIF) is the influencing design parameter. In general, it is difficult to quantify SIF for most of the practical applications. For simple geometries, SIF can be calculated by using handbooks (Rooke and Cartwright 1976, Murakami 1988). There is a need to evolve

*Corresponding author, Scientist, E-mail: murthyarc@serc.res.in, murthycsdg@gmail.com
[a]Student
[b]Scientist
[c]Director

Copyright © 2015 Techno-Press, Ltd.
http://www.techno-press.org/?journal=sem&subpage=8 ISSN: 1225-4568 (Print), 1598-6217 (Online)

efficient methodologies for computation of SIF and to provide an integrated approach that would include fatigue crack growth models for remaining life prediction. During the last four decades, a great deal of research (Poe 1971, Chu *et al.* 1982, Ghassem and Rich 1933, Wen *et al.* 2000, 2003, Saves *et al.* 2001, Dexter and Pilarsk 2002, Taheri *et al.* 2003, Mahmoud and Dexter 2005, Murthy *et al*. 2007, Liu *et al.* 2012, Hosseini *et al.* 2013) has been dedicated to the development of numerical/analytical methods for computation of SIF for stiffened and unstiffened plate panels subjected to uniaxial tensile stresses.

Fatigue tests were conducted by Poe (1971) on stiffened panels constructed with bolted and integral stringers. It was observed from the experiments that the bolted stringers reduced the crack growth rate significantly for a stressed unstiffened panel, whereas the integral stiffener had no significant effect. An experimental study was conducted by Chu *et al.* (1982) to characterize the fatigue crack growth behaviour of stiffened panels under uniform lateral pressure loading. A detailed explanation for the use of fracture diagram in the design of stiffened panels was presented by Ghassem and Rich (1933). Wen *et al.* (2000, 2003) employed dual boundary element method for a analysis of reinforced cracked shallow shells and SIFs were evaluated from crack opening displacements. These diagrams are useful for post-mortem failure analysis and in preventive quality control, whereby design measures may be taken to avoid failure. A simplified semi-analytical methodology was presented by Saves *et al.* (2001) to predict the behaviour of longitudinal cracks in cracked stiffened curved panels with frames. The results from this had a highly satisfactory correlation between prediction by calculation and experimental data. A series of experiments were conducted by Dexter and Pilarski (2002) to characterize the propagation of large fatigue cracks in welded stiffened panels under four point bending and observed that welded stiffeners substantially reduce the crack propagation rate relative to a plate with no stiffeners. It was found out that the effect of compressive residual stresses between the stiffeners reduces crack propagation rate. Mahmoud and Dexter (2005) conducted cyclic tension fatigue tests on approximately half-scale welded stiffened panels to study propagation of large cracks as they interact with the stiffeners. Analytical and FE models were developed based on the experimental results to assess the remaining life of ships with large cracks. Ramachandra Murthy *et al.* (2007) developed methodologies for remaining life prediction of stiffened panels under constant and variable amplitude loading. Liu *et al.* (2012) established a simple damage model based on the classical theory of damage and fracture mechanics. Hosseini-Toudeshky *et al.* (2013) employed the finite element method (FEM) to investigate the fracture analyses, crack growth trajectory and fatigue life of curved stiffened panels repaired with composite patches subjected to combined tension and shear cyclic loadings. It was shown that as the shear to tension ratio increases, the patch layups with orientations of almost perpendicular to the crack trajectory become more efficient in terms of fatigue crack growth life, when compared with the patch layups parallel to the tension orientation.

From the literature review, it is observed that the studies carried out on fracture analysis and remaining life prediction of stiffened panels by using fracture mechanics concepts is limited (Poe 1971, Chu *et al.* 1982, Ghassem and Rich 1933, Wen *et al.* 2000, 2003, Saves *et al.* 2001, Dexter and Pilarsk 2002, Taheri *et al.* 2003, Mahmoud and Dexter 2005, Rama Chandra Murthy *et al.* 2007, Liu *et al.* 2012, Hosseini *et al.* 2013, Papadakis 2013). Further, it is also observed that rigorous finite element analysis (FEA) needs to be performed to compute SIF for a structural component having complex geometry. In view of these, there is a need for development of analytical methodologies for fracture analysis and remaining life prediction of stiffened panels under fatigue loading. In this paper methodologies for fracture analysis and remaining life

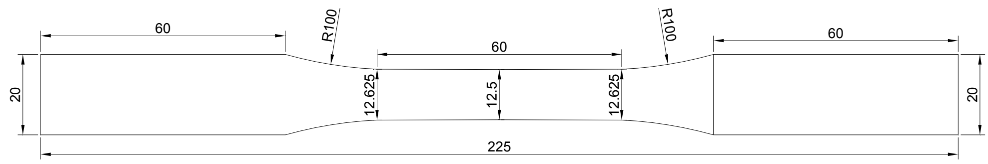

Fig. 1 Details of tension test specimen (All dimensions are in mm)

(a) Tension test set-up on aluminium alloy specimen

(b) Tension test specimens after failure

Fig. 2 Tension coupon specimen of Al 2014A

prediction of stiffened panels under fatigue loading have been proposed. SIF has been computed by using the domain integral technique available. Effect of concentric stiffeners made of various sizes and position on SIF and remaining life has been studied.

2. Experimental studies on Aluminium Alloy 2014A

Experiments have been carried out on aluminium alloy 2014A to evaluate mechanical parameters and crack growth constants. Tension coupon tests have been conducted as per ASTM B 557M - 10. Fig. 1 shows details of tension test specimens. The overall size of the specimen is 225×20×3 mm. Width at the reduced section is 12.5 mm. Instron fatigue rated universal testing machine (UTM) with capacity of ±250 kN has been used for conducting the tests. Extensometer of gauge length 50 mm is used to measure the change in strain over the gauge length. The test has been conducted under displacement control mode at 0.01 mm/sec. The gripping pressure is kept as 400 kips/inch^2. Fig. 2 shows the tension coupon specimen before and after testing. Various mechanical. Properties of Al 2014A are presented in Table 1. The average yield strength and ultimate tensile strength of the material are found to be 62 MPa and 84 MPa respectively. The Young's Modulus and % elongation of the material are found to be 71GPa and 10.7 respectively. Fig. 3 shows the typical stress-strain curve of aluminium alloy.

Fatigue crack growth (FCG) studies have been conducted on compact tension, C(T), specimens to determine the fatigue crack growth constants C and m for the aluminium alloy 2014A. Three specimens have been fabricated as per ASTM E 647 - 08. The overall size of the specimen is 62.5×60×3 mm. The initial notch length is 22.5mm. Fig. 4 shows details of a typical C(T) specimen. The required test fixtures for carrying FCG studies are also fabricated as per ASTM E

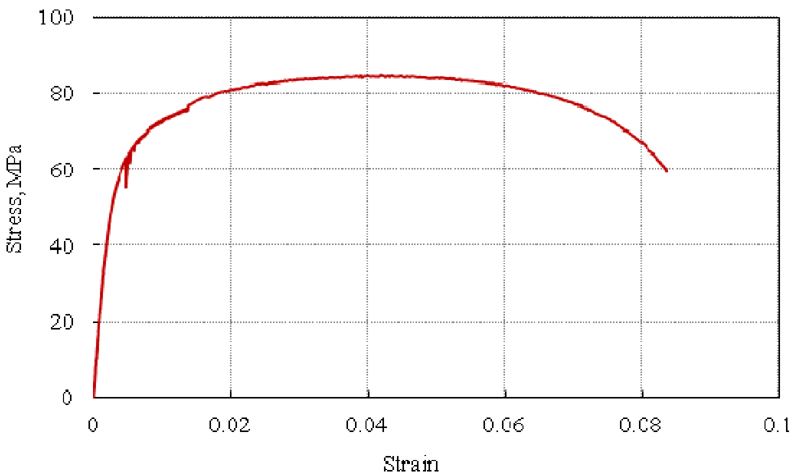

Fig. 3 Typical stress-strain curve of aluminium alloy

Table 1 Mechanical properties of Al 2014A

Mechanical Properties	Average value
Maximum load (N)	3154.78
Young's Modulus (N/mm^2)	71385
Yield Strength (N/mm^2)	61.67
Ultimate Strength (N/mm^2)	83.83
% elongation	10.67
% decrease in area	20.69

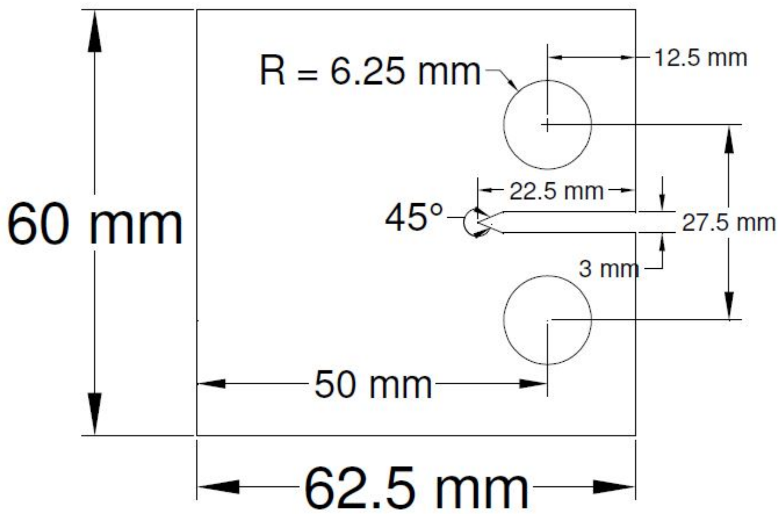

Fig. 4 Details of a typical C(T) specimen

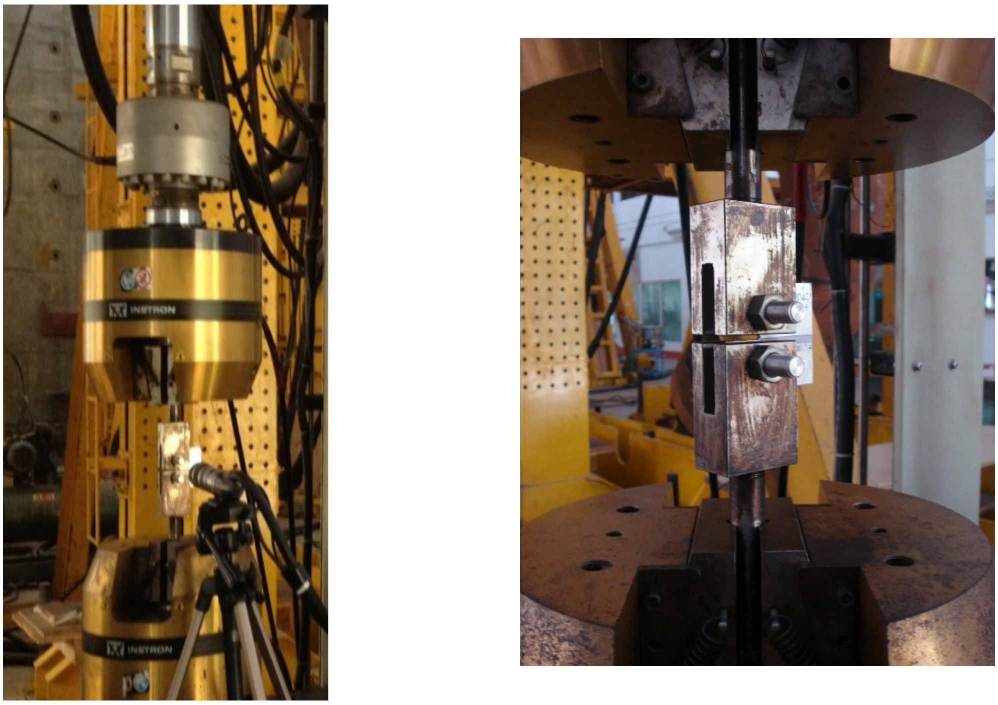

Fig. 5 Typical test setup of C(T) specimen

647. The tests have been conducted by using Instron fatigue rated UTM with capacity of ±250 kN under load control with a stress ratio, R=0.1 (tension-tension fatigue) with a frequency of 2.5–15 Hz. The tests have been conducted under constant amplitude fatigue load with a maximum load of 1kN and minimum load of 0.1 kN. The test frequency is varied between 2.5 Hz and 10 Hz and the

stress ratio is maintained as 0.1. Fig. 5 shows the typical test setup of compact tension specimen. Typical optical microscopy images of C(T) specimen are shown in Fig. 6. Optical measurements of crack extension at the surface and the corresponding number of fatigue cycles elapsed have been recorded for each of the C(T) tests. The number of cycles for crack initiation from v-notch varied from 88,000 to 1,65,000. The fatigue crack growth tests are continued till the crack length in these specimens reached approximately 20 mm.

For each specimen initiation life and total life have been recorded. Crack growth constants and fracture toughness have been evaluated as per standard procedure. Average values of test results are presented in Table 2.

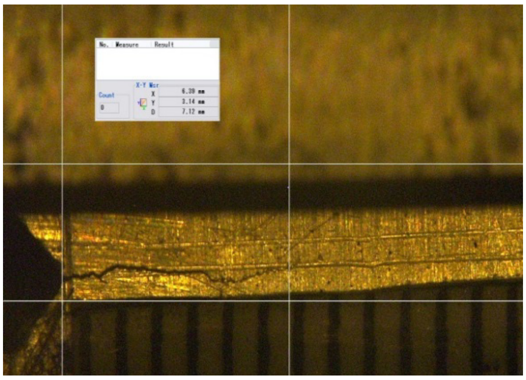

(a) at 400250 cycles

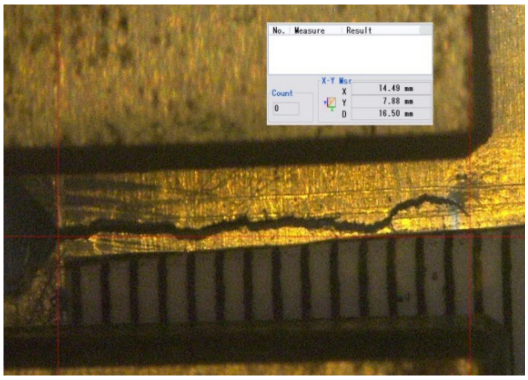

(b) at 586250 cycles

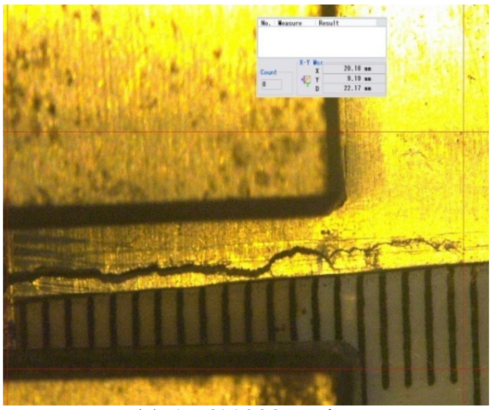

(c) At 611000 cycles

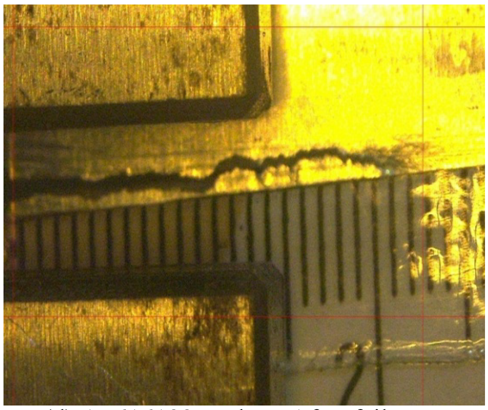

(d) At 616188 cycles - After failure

Fig. 6 Typical Optical microscopy images of C(T) specimen

Table 2 Compact tension specimen test results (Average)

Parameter	Average value	Parameter	Average value
Initiation life (N_i) from *v*-notch	140000	C	2.12E-10
Total life (N)	450654	m	3.14
Propagation life (N_p)	310654	Fracture toughness ($N/mm^2 \sqrt{m}$)	23.59

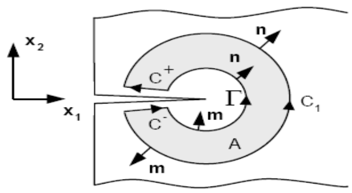

Fig. 7 Closed contour $C=C_1-\Gamma+C^{+}+C^{-}$ enclosing a simply connected region A

3. Computation of SIF

Computation of SIF is extremely difficult for the structures/ structural components having complex geometry. The prediction of the remaining life of a fatigue-damaged structure depends on a proper understanding of the crack growth behaviour, which in turn relies on the computation of SIF accurately. In this paper, the domain integral method available in ABAQUS software has been used to calculate the energy release, when a crack grows and convert it to SIF by relations between stresses and energy. Brief details of the method are given below.

3.1 The energy domain integral (Shih et al. 1986)

For stable crack growth in a two-dimensional body having a line crack along the x_1 axis, the strain energy release per unit crack advance is

$$J = \lim_{\Gamma\to 0}\int_{\Gamma}\left(W\delta_{1i} - \sigma_{ij}u_{j,1}\right)n_i\,dC \tag{1}$$

where W is the stress work density, σ_{ij} and u_i are components of the stress and displacement along the x_i axis, n_i is the unit vector normal to Γ contour and dC is the infinite tesimal arc length as depicted in Fig. 7.

In the absence of thermal strain, body force and crack face traction, Eq. (1) can be expressed in the form

$$J = \int_{c}\left[\sigma_{ij}u_{j,1} - W\delta_{1i}\right]m_i q_1\,dC \tag{2}$$

where $C=C_1+C^{+}+C^{-}-\Gamma$ is the closed curve, q_1 is a sufficiently smooth function in the area enclosed by C, which is unity on Γ and zero on C_1, and m_j is the components of outward normal unit vector as shown in Fig. 5. By applying the divergence theorem to Eq. (2)

$$J = \int_{A}\left[\left(\sigma_{ij}u_{j,1} - W\delta_{1\tau}\right)q_1\right]_1 dA \tag{3}$$

where A is the area enclosed by C. Invoking the equilibrium equation, the domain expression for the energy release rate is

$$\mathrm{J} = \int_{\mathrm{A}}\left[\sigma_{ij}\mathrm{u}_{j,1} - \mathrm{W}\delta_{1i}\right]\mathrm{q}_{1,j}\,\mathrm{dA} \tag{4}$$

The function q_1 can be interpreted as a unit translation on Γ in the x_1 direction, while keeping the material points on C_1 fixed. According to the vanishing of Γ around the tip, this can be viewed as the growth of the crack.

In linear elastic material response, SIF in opening mode can be computed from the strain energy release rate (SERR) by the expression

$$K_I = \sqrt{J E'} \tag{5}$$

where $E' = E$, and $\frac{E}{1-\nu^2}$ for plane stress and plane strain case respectively, E is the modulus of elasticity, and ν is the Poisson's ratio.

3.2 Finite element formulation for the domain integral method

For the six-node isoparametric element, the coordinates, displacements and a smooth function are

$$x_i = \sum_{k=1}^{6} N_k X_{ik} \tag{6}$$

$$u_i = \sum_{k=1}^{6} N_k U_{ik} \tag{7}$$

$$q_1 = \sum_{k=1}^{6} N_k Q_{1k} \tag{8}$$

where N_k are the shape functions, X_{ik} are the nodal coordinates, U_{ik} are the nodal displacements and Q_{1k} are the nodal values of the smooth function varying between 1 and 0. Using Eqs. (6) and (8) and the chain rule, the spatial gradient of q_1 is

$$\frac{\partial q_1}{\partial x_j} = \sum_{i=1}^{6} \sum_{k=1}^{2} \frac{\partial N_1}{\partial \eta_k} \frac{\partial \eta_k}{\partial x_j} Q_{11} \tag{9}$$

where $\frac{\partial \eta_k}{\partial x_j}$ is the inverse jacobian matrix.

For 2×2 Gaussian integration, the energy release rate expression in Eq. (2) is

$$J = \sum_{\substack{all \\ elements \\ in\ A}} \sum_{p=1}^{4} W_p \left\{ \left[\sigma_{ij} \frac{\partial u_j}{\partial x_1} - W \delta_{1i} \right] \frac{\partial q_1}{\partial x_1} \det\left(\frac{\partial x_k}{\partial \eta_k} \right) \right\}_p t \tag{10}$$

where all quantities are calculated at the 4 Gauss points with W_p as their respective weights and t is the specimen thickness.

In the present study a four noded bi linear element (CPS4) available in ABAQUS software is used to model the plate and crack. A 2×2 gauss quadrature with 4 gauss points are used to numerically evaluate the integral in Eq. (4). The finite element implementation of Eq. (4) is as follows.

1. Consider the inner contour closer to the crack tip.
2. Define the radius of the outer contour and identify the elements which are within the radius and cut by the outer contour. This forms the domain of elements for the computation of domain integral.
3. At each gauss point of the element, within the domain, compute the integrand defined in Eq. 4 and cumulatively add the result for the entire domain of elements, which results in J integral value

3.3 Remaining life prediction

Analysis of fatigue crack growth and remaining life prediction involves obtaining several data in relation to the loading conditions, type of material and crack geometry. A suitable crack growth law used is given below.

$$\frac{da}{dN} = f(\Delta K, R, ...) \tag{11}$$

The number of loading cycles required to extend the crack from an initial length a_0 to the final critical crack length a_f is given by

$$N = \int_{a_0}^{a_f} \frac{da}{f(\Delta K, R, ...)} \tag{12}$$

The remaining life prediction by using eqn. 12 involves calculating the integral and the procedure to be used depends, among other factors, on the type of load involved. The cycle-by-cycle approach involves calculating the number of cycles for each crack length increment.

4. Numerical studies

4.1 Studies on Al 2014A

SIF has been computed for Al 2014A centre cracked panels with and without stiffeners under uniaxial tensile load by using FEM. ABAQUS software has been used for fracture analysis. Various stiffener sizes and position of stiffeners have been considered in the analysis. The data/ information related to the aluminium panel made of 2014A is given in Table 3. Typical stiffened panel is shown in Fig. 8.

Fracture analysis has been carried out for various stiffener sizes and positions. Bilinear element (CPS4) available in ABAQUS has been employed for modelling. The total number of elements and nodes for a typical case are 12113 and 17654 respectively. Figs. 9 and 10 show the typical finite element model of Al 2014A and typical stress contour (S22) corresponding to stiffener size 12 mm^2 and stiffener position is at edge. Figs. 11 and 12 show the typical stress contour in y-direction (S22) for the same stiffener size, but stiffeners are at 0.567W and 0.233W from centre of the panel respectively.

Table 3 Data/Information of Al 2014A panel

Dimensions (height, 2H×width, 2W× thickness, t)	250×150×3 mm	Crack growth model	Paris
Max. Stress	30.8 MPa	C	2.12e-10
Fracture toughness	23.59 MPa√m	m	3.14
Yield strength	61.67 MPa	Stiffener area (mm^2)	12,18,24,30
Stress condition at crack tip and Initial crack length	plane stress, 7.5mm	Stiffener position (Xs)	Edge, 0.567W, 0.233W (W=Half width of the panel)

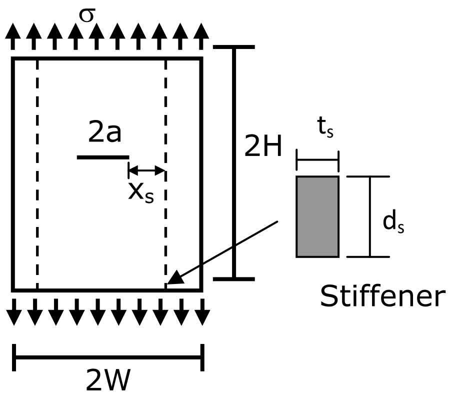

Fig. 8 Typical stiffened panel

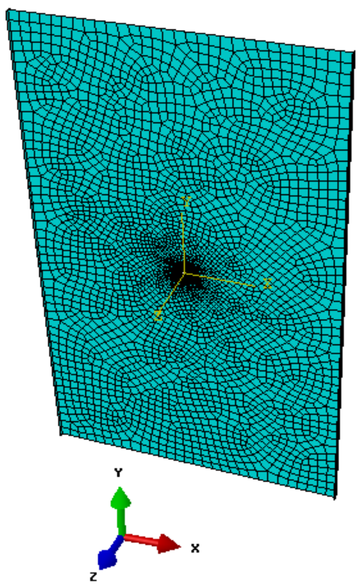

Fig. 9 Typical FE model (Stiffener at edge)

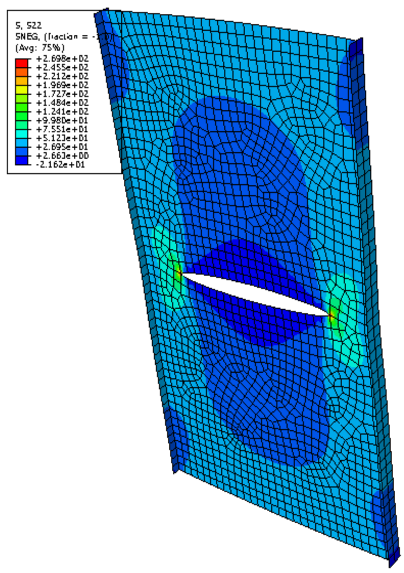

Fig. 10 Stress contour – σ 22 (stiffener at edge)

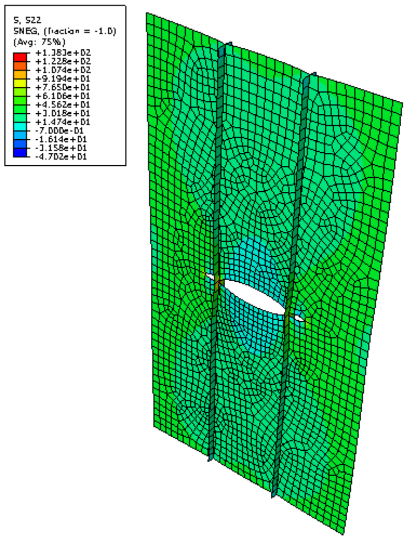

Fig. 11 Stress contour – S22 (Stiffener at 25 mm from centre)

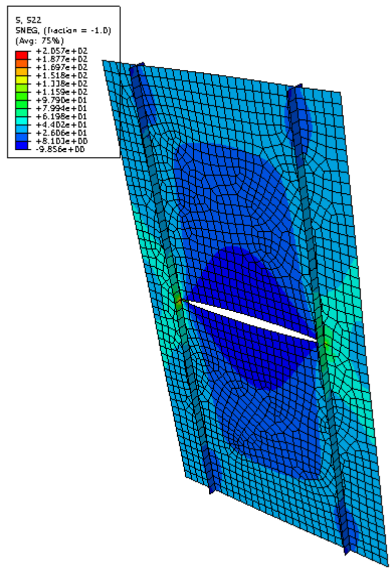

Fig. 12 Stress contour – S22 (Stiffener at 50 mm from centre)

Table 4 Comparison of SIFs for Unstiffened 2014A panel

Half crack length, a (mm)	SIF, K, (MPa√m)	
	Present study	Analytical results (Rooke and Cartwright 1976)
7.5	4.74	4.75
10	5.51	5.52
15	6.85	6.86
20	8.07	8.08
25	9.28	9.27
30	10.55	10.51
35	11.90	11.85
40	13.41	13.35
45	15.19	15.10
50	17.38	17.26

Table 4 shows the comparison of SIF of unstiffened 2014A with the analytical results available in the literature (Rooke and Cartwright 1976). It can be observed from Table 4 that SIF computed by using FEA is in very good agreement with that the analytical results of Rooke and Cartwright (1976).

Table 5 presents the results of SIF obtained in the present study for various crack lengths and stiffener areas for the case of edge stiffened case. Along with analytical results available in the literature (Rooke and Cartwright 1976). From Table 5, it can be noted that SIF computed in the present study is in very good agreement with that of corresponding analytical results available in the literature. This validates the proposed methodology for fracture analysis of stiffened panels. Tables 6 and 7 presents SIF obtained for Al 2014A for the case of stiffened plate with stiffener

Table 5 SIF for edge stiffened panels for 2014A

Half Crack length, a_0 (mm)	SIF, K, (MPa√m)							
	Stiffener area 12 mm^2		Stiffener area 18 mm^2		Stiffener area 24 mm^2		Stiffener area 30 mm^2	
	Present Study	Analytical results (Rooke and Cartwright 1976)	Present Study	Analytical results (Rooke and Cartwright 1976)	Present Study	Analytical results (Rooke and Cartwright 1976)	Present Study	Analytical results (Rooke and Cartwright 1976)
7.5	4.63	4.81	4.58	4.76	4.57	4.73	4.52	4.67
10	5.31	5.66	5.26	5.63	5.18	5.52	5.11	5.42
15	6.57	6.91	6.45	6.87	6.35	6.69	6.26	6.58
20	7.78	8.03	7.63	7.97	7.51	7.89	7.39	7.67
25	8.88	9.23	8.70	9.13	8.54	9.01	8.40	8.86
30	10.05	10.36	9.83	10.14	9.64	9.93	8.99	9.36
35	11.28	11.67	11.01	11.38	10.76	11.11	10.53	10.89
40	12.66	12.94	12.32	12.74	12.01	12.44	11.73	12.14
45	14.13	14.42	13.69	14.12	13.30	13.76	12.94	13.45
50	15.95	16.54	15.33	15.83	14.88	15.34	14.42	14.83

Table 6 SIF for Intermediate stiffened plate (X_s=0.567W)

Half crack length, a_0 (mm)	SIF, K, (MPa√m)			
	Stiffener area 12 mm^2	Stiffener area 18 mm^2	Stiffener area 24 mm^2	Stiffener area 30 mm^2
7.5	4.47	4.28	4.20	4.18
10	5.19	5.17	5.06	4.95
15	6.50	6.35	6.20	6.06
20	7.69	7.50	7.32	7.15
25	8.77	8.54	8.32	8.11
30	9.91	9.62	9.34	9.09
35	11.08	10.70	10.36	10.05
40	12.40	11.93	11.49	11.10
45	13.64	13.01	12.45	11.94
50	14.79	13.91	13.12	12.49

position at X_s=0.576W and X_s=0.233W respectively. A best fit has been obtained by using MATLAB software for the data of SIF values of various stiffener sizes, crack lengths and positions. Various parametric equations including norm of residuals have been generated by using MATLAB and are presented in Table 8.

From Tables 5 to 7, the following are obtained , as expected (i) SIF is increasing with increase of crack length for a particular stiffener size (ii) with increase of stiffener size, SIF is decreasing for a given crack length and (iii) SIF is increasing with the increase of distance of stiffener from the crack tip.

Table 7 SIF for intermediate stiffened plate (X_s= 0.233W)

Half crack length, a_0 (mm)	SIF, K, (MPa√m)			
	Stiffener area 12 mm^2	Stiffener area 18 mm^2	Stiffener area 24 mm^2	Stiffener area 30 mm^2
7.5	4.31	4.25	4.23	4.08
10	5.01	5.07	4.91	4.78
15	6.35	6.14	5.94	5.75
20	7.43	7.13	6.87	6.63
25	8.16	7.75	7.26	6.96
30	7.88	7.41	7.17	6.74
35	7.91	7.37	7.04	6.65
40	8.03	7.43	6.94	5.90
45	8.54	7.87	7.14	6.07
50	8.94	8.18	7.37	6.99

Table 8 Parametric equation for computation of SIF

Stiffener area (mm^2)	**Stiffener position**	**Equation for SIF, K** (MPa√m)	**Norm of residuals**
0	**unstiffened**	$45x^3-39x^2+30x+2.1$	0.0548
12	**edge**	$31x^3-29x^2+0.24x+2.3$	0.0565
18	**edge**	$25x^3-24x^2+24x+2.4$	0.0533
24	**edge**	$23\,x^3-23x^2+23x+2.4$	0.06485
30	**edge**	$-78x^4+140x^3-85x^2+35x+1.7$	0.0378
12	**Intermediate, *Xs*=0.567W**	$-91x^4+150x^3-86x^2+37x+1.5$	0.061
18	**Intermediate, *Xs*=0.567W**	$-130x^4+210x^3-120x^2+43x+0.96$	0.103
24	**Intermediate, *Xs*=0.567W**	$-140x^4+220x^3-20x^2+43x+0.92$	0.1
30	**Intermediate, *Xs*=0.567W**	$-120x^4\ +190x^3-100x^2+38x+1.2$	0.0832
12	**Intermediate, *Xs*=0.233W**	$72x^4-27x^3-56x^2+40x+0.77$	0.4799
18	**Intermediate, *Xs*=0.233W**	$43x^4\ +16x^3-76x^2+42x+0.74$	0.0457
24	**Intermediate, *Xs*=0.233W**	$77x^4-49x^3-35x^2+31x+1.4$	0.2523
30	**Intermediate, *Xs*=0.233W**	$300x^4-350x^3\ +110x^2+56x+0.28$	0.288

where, X_S=distance from crack tip and x=ratio of half crack length to half plate width

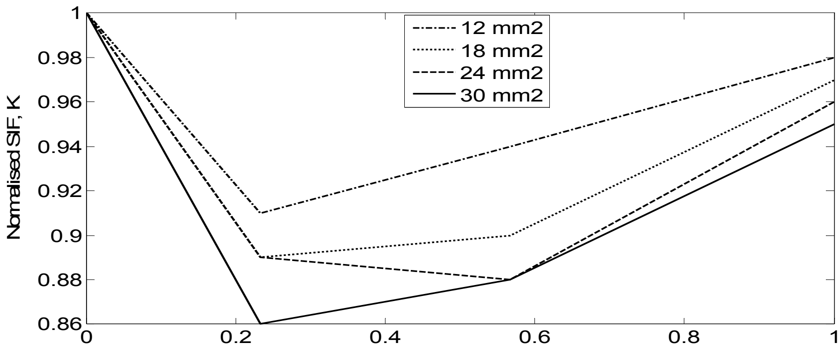

Normalised stiffener position w.r.t half plate width

Fig. 13 (a) Normalised stiffener position vs normalised SIF (a=7.5 mm)

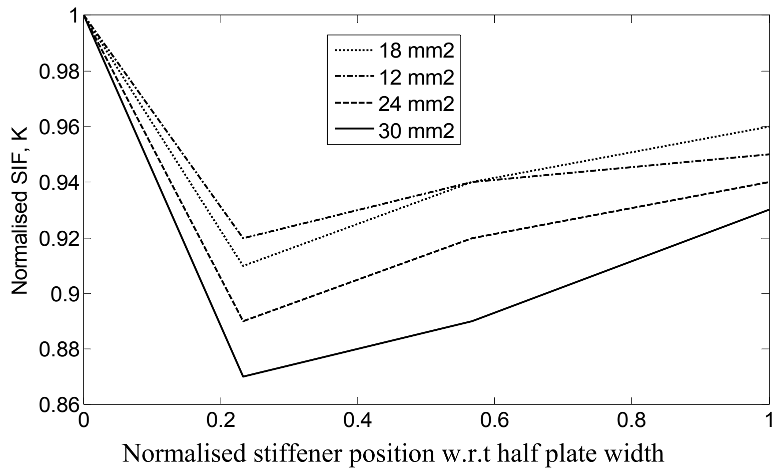

Fig. 13 (b) Normalised stiffener position vs normalised SIF (a=10 mm)

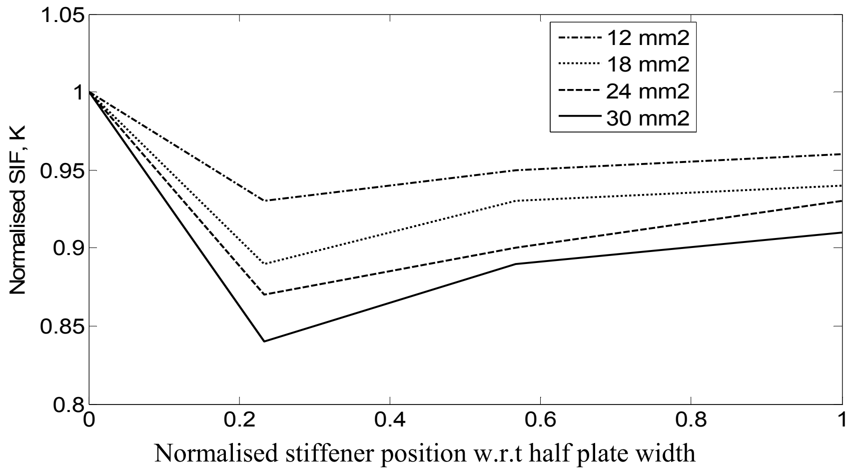

Fig. 13 (c) Normalised stiffener position vs normalised SIF (a=15 mm)

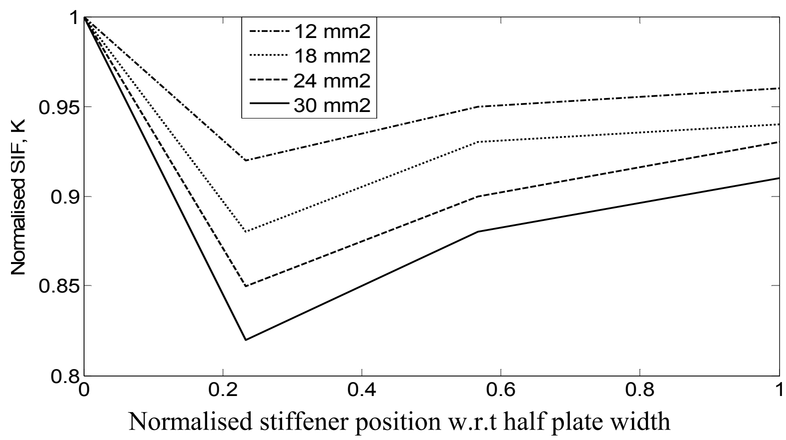

Fig. 13 (d) Normalised stiffener position vs normalised SIF (a=20 mm)

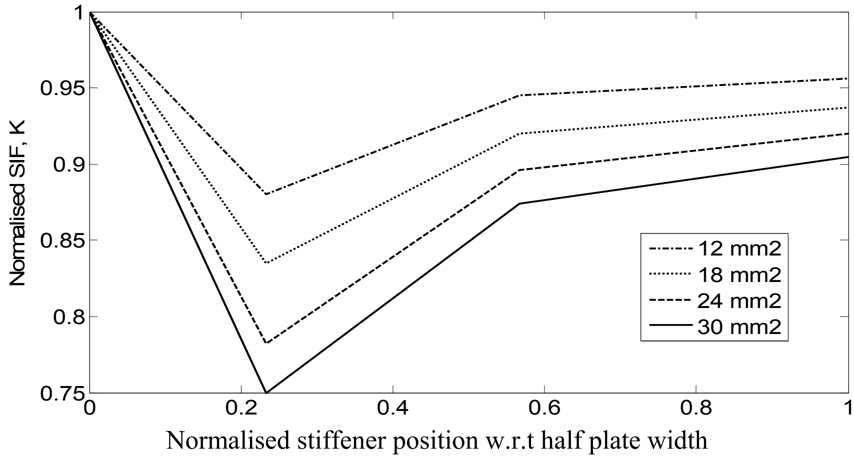

Fig. 13 (e) Normalised stiffener position vs normalised SIF (*a*=25 mm)

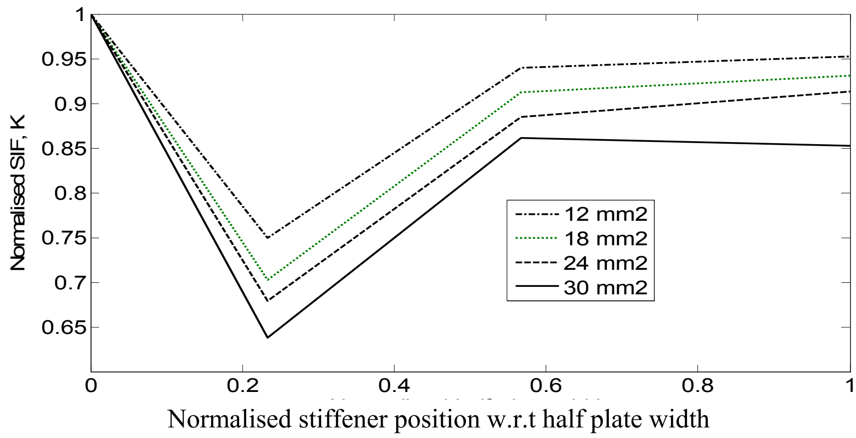

Fig. 13 (f) Normalised stiffener position vs normalised SIF (*a*=30 mm)

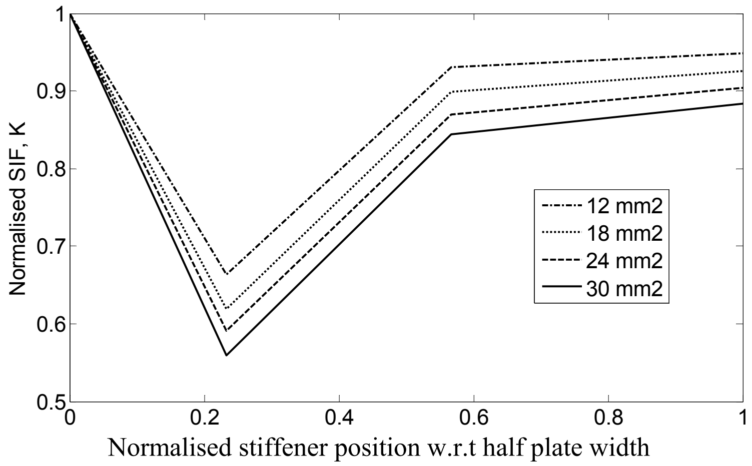

Fig. 13 (g) Normalised stiffener position vs normalised SIF (*a*=35 mm)

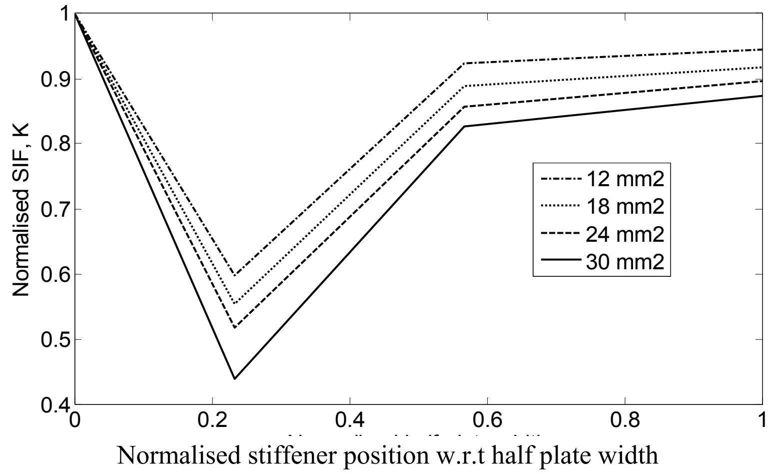

Fig. 13 (h) Normalised stiffener position vs normalised SIF (*a*=40 mm)

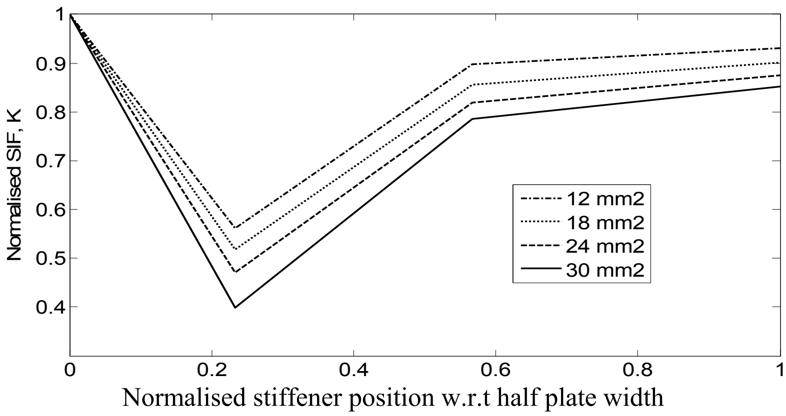

Fig. 13 (i) Normalised stiffener position vs normalised SIF (*a*=45 mm)

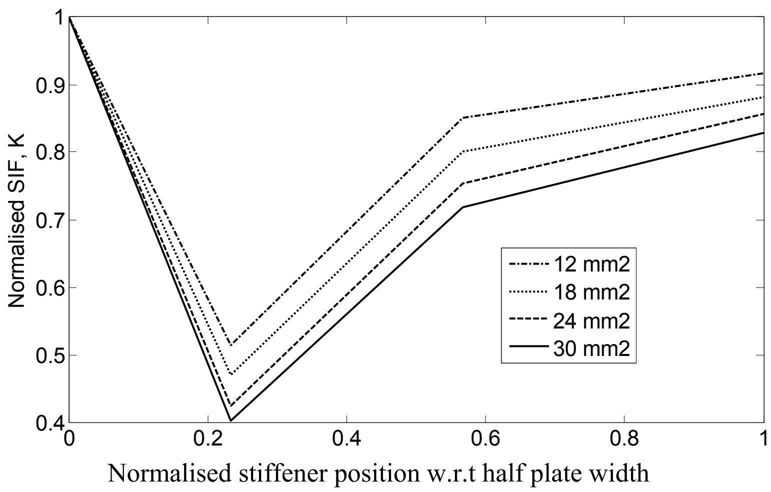

Fig. 13 (j) Normalised stiffener position vs normalised SIF (*a*=50 mm)

Fig. 13 (a) to (j) presents the variation of SIF with stiffener position for various crack lengths and stiffener sizes. From Fig. 13 (a) to (j), it can be observed that the trend is similiar for all the stiffener sizes w.r.t position of stiffener. These above parametric equations and curves will be readily useful to determine SIF at any position of stiffener and for stiffener size by appropriately interpolating the values of ascending and descending portion of the plot.

Crack growth studies and remaining life prediction has been carried out for all the cases by using the parametric equations presented above. Paris crack growth model has been used for remaining prediction

$$\frac{da}{dN} = C(\Delta K)^m \tag{13}$$

Figs. 14 to 16 show the variation of remaining life with crack length corresponding to various stiffener sizes and stiffener locations.

From Figs. 14 and 15, it can be observed that the predicted remaining life of stiffened panel under fatigue loading increases with increase of stiffener area and the percentage increase is very significant for the higher stiffener areas compared to the unstiffened case. Further, it can also be observed that the remaining life of concentric stiffened panel increases as the position of stiffener is closer to the crack tip compared to unstiffened case and away from the crack tip.

Table 9 presents the predicted remaining life values of stiffened panel for various stiffener sizes and position of stiffeners.

From Table 9, it can be observed that the predicted normalised remaining life for the case of edge stiffened panel is 1.16, 1.21, 1.27 and 1.48 for stiffener sizes 12, 18, 24 and 30 mm^2 respectively compared to unstiffened case. For the stiffener position at 0.567 W, the predicted

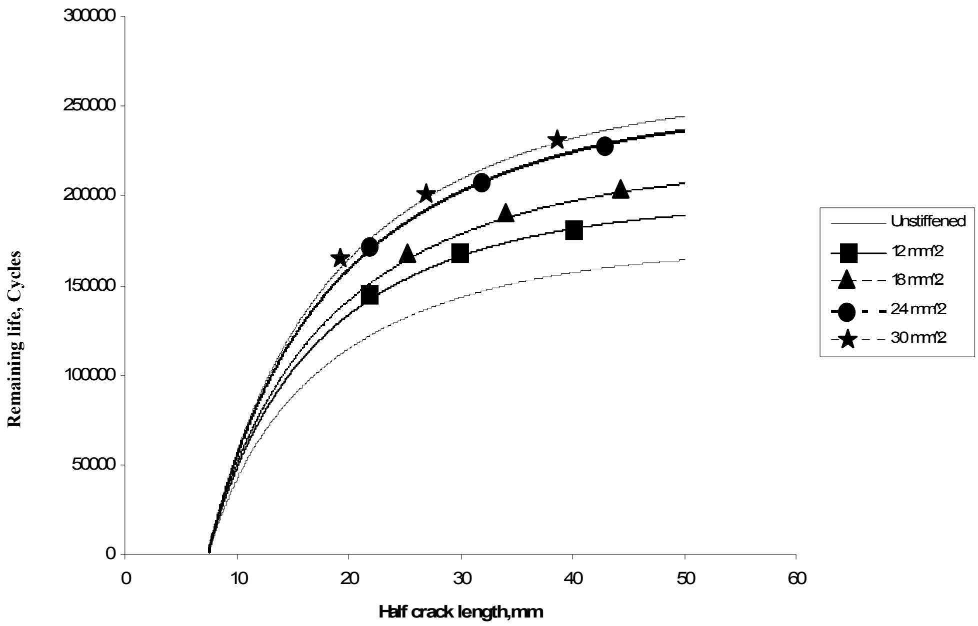

Fig. 14 Variation of remaining life with crack length (stiffener position is at edges)

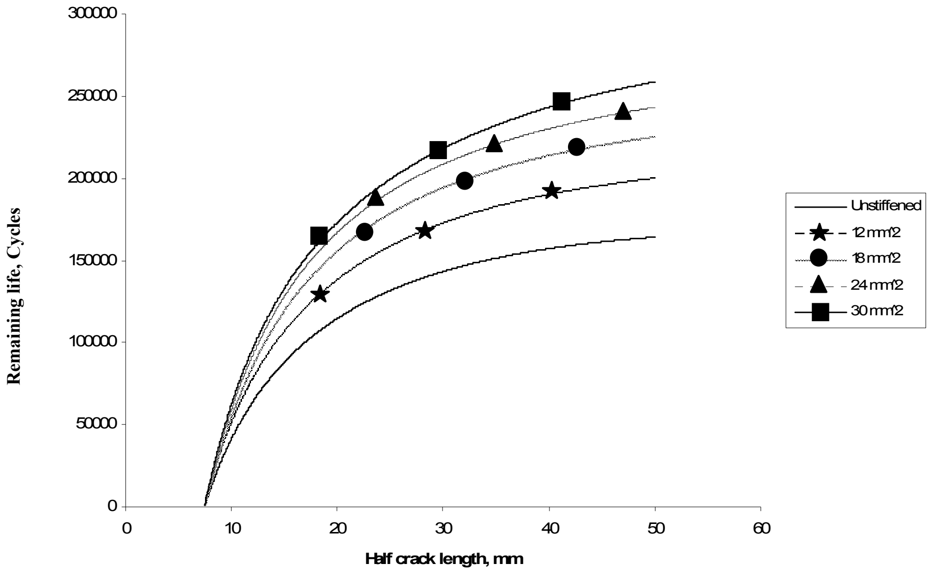

Fig. 15 Variation of remaining life with crack length (stiffener position is at 0.567W)

Table 9 Remaining life for a plate with concentric stiffener – Al 2014 A

Stiffener area (mm^2)	Stiffener position	Predicted remaining life	Normalised remaining life w.r.t unstiffened case
-	Unstiffened	258587	1
12	Edge	300323	1.16
18	Edge	314064	1.21
24	Edge	328258	1.27
30	Edge	382943	1.48
12	X_s=0.567W	320453	1.24
18	X_s=0.567W	350822	1.36
24	X_s=0.567W	380479	1.47
30	X_s=0.567W	404452	1.56
12	X_s=0.233W	444585	1.72
18	X_s=0.233W	498194	1.93
24	X_s=0.233W	587238	2.27
30	X_s=0.233W	714149	2.76

normalised remaining life is 1.24, 1.36, 1.47 and 1.56 for stiffener sizes 12, 18, 24 and 30 mm^2 respectively compared to unstiffened case. Similarly, for the stiffener position at 0.233 W, the predicted normalised remaining life is 1.72, 1.93, 2.27 and 2.76 for stiffener sizes 12, 18, 24 and 30 mm^2 respectively compared to unstiffened case. Fig. 16 shows the variation of remaining life w. r. t stiffener position and size. This graph will be readily useful for prediction of remaining life of stiffened panel for various stiffener sizes and positions. This graph will further be useful for damage tolerant design of structural components subjected to fatigue loading.

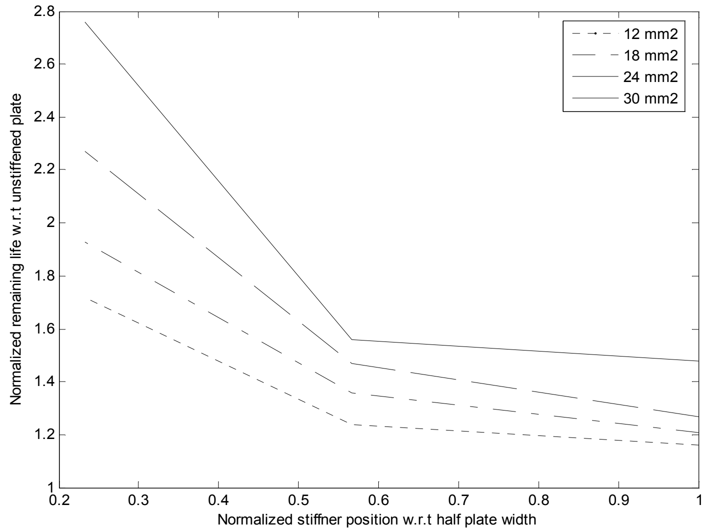

Normalised stiffener position

Fig. 16 Variation of remaining life w.r.t stiffener position and size

Table 10 Data/Information of 350 WT Steel

Dimensions (height×width×thickness)	250×150×3 mm	Crack growth model	Paris
Max. stress	114 MPa	C	1.02e-8
Fracture toughness	50 MPa√m	m	2.94
Yield strength	350 MPa	Stiffener areas (mm^2)	12,18,24,30
Stress condition at crack tip and Initial crack length	plane stress, 7.5 mm	Stiffener position (*Xs*)	Edge and 0.567W, 0.233W (W=Half width of the panel)

Table 11 Remaining life for plate with a concentric stiffener – 350 WT steel

Stiffener area (mm^2)	Stiffener position	Predicted remaining life	Normalised remaining life w.r.t unstiffened case
-	Unstiffened	164217*	1
12	Edge	189040	1.15
18	Edge	206231	1.23
24	Edge	236407	1.27
30	Edge	244343	1.48
12	X_s=0.567W	199676	1.21
18	X_s=0.567W	225614	1.37
24	X_s=0.567W	243273	1.48
30	X_s=0.567W	258720	1.57
12	X_s=0.233W	284868	1.73
18	X_s=0.233W	326537	1.93
24	X_s=0.233W	386972	2.29
30	X_s=0.233W	445896	2.71

* - 156000 cycles (Experimental value (Taheri *et al.* 2003))

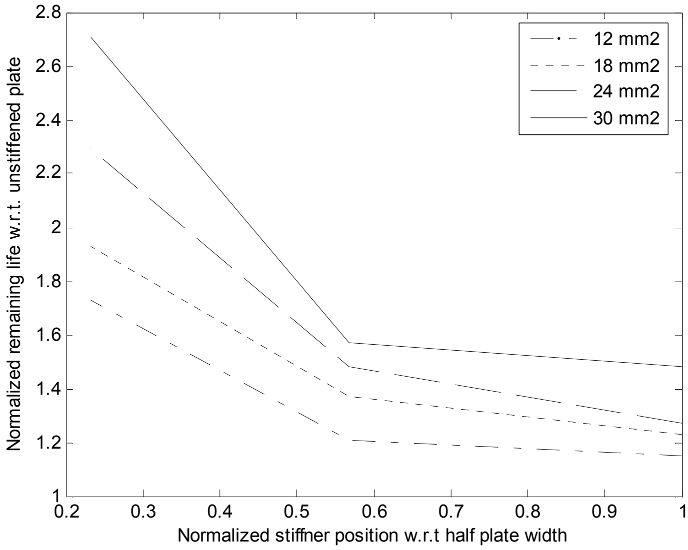

Normalised stiffener position

Fig. 17 Variation of remaining life w.r.t to stiffener position and size – 350WT Steel

4.2 Studies on 350 WT Steel

Fracture analysis and remaining life prediction has been carried out for 350 WT steel with the information given in Table 10. Material properties and crack growth constants have been taken from literature (Taheri *et al.* 2003). Table 11 shows the predicted remaining life w.r.t stiffener position for various stiffener sizes.

From Table 11, it can be observed that the predicted normalized remaining life for the case of edge stiffened panel is 1.15, 1.23, 1.27 and 1.48 for stiffener sizes 12, 18, 24 and 30 mm^2 respectively compared to unstiffened case. For the stiffener position at 0.567 W, the predicted normalised remaining life is 1.21, 1.37, 1.48 and 1.57 for stiffener sizes 12, 18, 24 and 30 mm^2 respectively compared to unstiffened case. Similarly, for the stiffener position at 0.233 W, the predicted normalised remaining life is 1.73, 1.93, 2.29 and 2.71 for stiffener sizes 12, 18, 24 and 30 mm^2 respectively compared to unstiffened case. Fig. 17 shows the variation of remaining life w. r. t stiffener position and size. This graph will be readily useful for prediction of remaining life of stiffened panel for various stiffener sizes and positions. This graph will further be useful for damage tolerant design of structural components subjected to fatigue loading.

From Tables 9 and 11, it can be observed that the normalised remaining life is same for a known stiffener position and size irrespective of the material. However, the material information of respective material has been taken care of in the prediction of remaining life of unstiffened panel. The material information include the crack growth constants, fracture toughness, yield strength etc. An important observation can be drawn from overall study is that, one can estimate the remaining life for stiffened panel for particular stiffener size and position by knowing the remaining life of unstiffened panel. For other metals, the remaining life of stiffened panel can be predicted by appropriately incorporating the material properties in the prediction of remaining life of the unstiffened panel for a given crack length.

5. Conclusions

Towards damage tolerant design, fracture analysis and remaining life prediction of aluminium alloy 2014A plate panels with concentric stiffener has been carried out under fatigue loading. Various mechanical properties and crack growth constants have been evaluated for Al 2014A by conducting tension coupon and compact tension tests. Various stiffener sizes and position of stiffener have been considered as primary variables in this study. One of the important fracture parameter, SIF, has been computed for various cases by using domain integral technique available in ABAQUS, FEA software. SIF has been obtained for various crack lengths and stiffener sizes and position of stiffeners. The best fit equation for computation of SIF has been obtained by employing MATLAB software. Remaining life has been predicted by using Paris crack growth model. From the studies, it is observed that the remaining life of the stiffened panels is significantly higher compared to unstiffened panels. It is also observed that the remaining life increases as the stiffener size increases and is very high when the stiffener position is close to crack tip. Normalised remaining life is predicted for various stiffener positions and stiffener sizes for two materials, namely, Al 2014A and 350 WT steel. It has been observed that the normalised remaining life is same for a known stiffener position and size irrespective of the material. However, the material information of respective material has been taken care of in the prediction of remaining life of unstiffened panel. The material information include the crack growth constants, fracture toughness, yield strength etc. An important observation can be drawn from overall study is that, one can estimate the remaining life for stiffened panel for particular stiffener size and position by knowing the remaining life of unstiffened panel. For other metals, the remaining life of stiffened panel can be predicted by appropriately incorporating the material properties in the prediction of remaining life of the unstiffened panel for a given crack length.

Acknowledgements

Authors acknowledge the technical discussions and support provided by Computational Structural Mechanics Group of CSIR-SERC. Authors also thanks aeronautics R&D Board (AR & DB), New Delhi for partial grant towards this investigations. This paper is being published with the permission of Director, CSIR-SERC.

References

ASTM B 557M - 10, Standard test methods for tension testing of wrought and cast aluminium- & magnesium-alloy products.

ASTM B 557M - 10, Standard Test Methods for Tension Testing of Wrought and Cast Aluminum- and Magnesium- Alloy Products (Metric), ASTM International, USA.

ASTM E 647 - 08, Standard test method for measurement of fatigue crack growth rates.

ASTM E 647 - 11, Standard Test Method for Measurement of Fatigue Crack Growth Rates, ASTM International, USA.

Chu, H.P., Hauser, J.A. and Sikoram, J.P. (1982), "Fatigue crack growth in stiffened panels under pressure loading-design of fatigue and fracture resistant structures", *ASTM STP*, **761**, 345-72.

Dexter, R.J. and Pilarski, P.J. (2002), "Crack propagation in welded stiffened panels", *J. Constr. Steel Res.*, **58**, 1081-102.

Ghassem, M.M. and Rich, T.P. (1933), "The fracture diagram: a new design tool for stiffened panels", *AIAA J.*, 21.

Hosseini-Toudeshky, H., Ghaffari, M.A. and Mohammadi, B. (2013), "Mixed-mode crack propagation of stiffened curved panels repaired by composite patch under combined tension and shear cyclic loading", *Aerosp. Sci. Technol.*, **28**(1), 344-363.

Liu, G., Wang, S. and Yang, X. (2012), "A Simple numerical simulation of crack growth rate", *Procedia Eng.*, **31**, 557-562.

Mahmoud, H.N. and Dexter, R.J. (2005), "Propagation rate of large cracks in stiffened panels under tension loading", *Marin. Struct.*, **18**(3), 265-288.

Murakami, Y. (1988), *Stress intensity factors handbook*, Pergamon Press, Oxford.

Murthy, R.A., Palani, G.S. and Iyer, N.R. (2007), "Remaining life prediction of cracked stiffened panels under constant and variable amplitude loading", *Int. J. Fatig.*, **29**(6), 1125-1139.

Papadakis, V.G. (2013), "Service life prediction of a reinforced concrete bridge exposed to chloride induced deterioration", *Adv. Concrete Construct.*, **1**(3), 201-213.

Poe, Jr. C.C. (1971), "Fatigue propagation in stiffened panels", *ASTM STP*, **486**, 79-98.

Rooke, D.P. and Cartwright, D.J. (1976), *Compendium of stress intensity factors*, Her Majesty's Stationary Office, London.

Saves, C.S.T., Germes Davy, A. and Barrau, J.J. (2001), "Prediction of the longitudinal crack behaviour of stiffened curved panels", *Int. J. Fatig.*, **23**, 147-58.

Shih, C.F., Moran, B. and Nakamura, T. (1986), "Energy release rate along a three - dimensional crack front in a thermally stressed body", *Int. J. Fract.*, **30**, 79-102.

Taheri, F., Trask, D. and Pegg, N. (2003), "Experimental and analytical investigation of fatigue characteristics of 350WT steel under constant and variable amplitude loadings", *Marin. Struct.*, **16**, 69-91.

Wen, P.H., Aliabadi, M.H. and Young, A. (2000), "Stiffened cracked plates analysis by dual boundary element method", *Int. J. Fract.*, **106**, 245-258.

Wen, P.H., Aliabadi, M.H. and Young, A. (2003), "Fracture mechanics analysis of curved stiffened panels using BEM", *Int. J .Solids Struct.*, **40**(1), 219-236

CC